Supramolecular photocatalysts fixed on the inside of polypyrrole layer in dye-sensitized molecular photocathodes: application to photocatalytic CO_2 reduction coupled with water oxidation

Fazalurahman Kuttassery,[1,†] Hiromu Kumagai,[2] Ryutaru Kamata,[1] Yusuke Ebato,[1] Masanobu Higashi,[3] Hajime Suzuki,[4] Ryu Abe, [4] and Osamu Ishitani*,[1]

[1] Department of Chemistry, Tokyo Institute of Technology, 2-12-1-NE-1, O-okayama, Meguro-ku, Tokyo 152-8550, Japan.

[2] Institute of Multidisciplinary Research for Advanced Materials, Tohoku University, 2-1-1, Katahira, Aoba-ku, Sendai, Miyagi 980-8577, Japan.

[3] The OCU Advanced Research Institute for Natural Science and Technology Osaka City University, 3-3-138 Sugimoto, Sumiyoshi-ku, Osaka City, Osaka, 558-8585, Japan.

[4] Department of Energy and Hydrocarbon Chemistry, Graduate School of Engineering, Kyoto University, Katsura, Nishikyo-ku, Kyoto 615-8510, Japan.

[†] Present address: Department of Chemistry, University of Calicut, Malappuram, Kerala 673635, India.

Supplementary information

SI - I Synthetic strategy and ^{1}H-NMR Spectra of ligands and Ru(II) Complexes

(a) 4,4'-bis((1H-pyrrol-1-yl)methyl)-2,2'-bipyridine (Pyrdmb)
(b) [Ru(dmb)2]Cl_2
(c) [Ru(Pyrdmb)$_2$$Cl_2$]
(d) [Ru(dmb)(Pyrdmb)Cl_2]
(e) [Ru(dmb)$_2$(Pyrdmb)]$(PF_6)_2$ (PyrRu)
(f) [Ru(Pyrdmb)$_2$(dmb)]$(PF_6)_2$ (Pyr2Ru)
(g) [Ru(dmb)(Pydmb)(dmb-PO_3H_2)]$(PF_6)_2$ (PRuPyr)
(h) [Ru(dmb)(Pydmb)(bpyC_2bpy)]$(PF_6)_2$ (PyrRuC_2bpy)
(i) [Ru(dmb)(Pydmb)(bpyC_2bpy)Ru(CO)$_2$$Cl_2$]$(PF_6)_2$ (PyrRuC_2RuCAT)

SI - II Figures, Schemes and Tables

SI – I Synthesis and Characterization of metal complexes

(a) ***Synthesis of 4,4'-bis((1H-pyrrol-1-yl)methyl)-2,2'-bipyridine (Pyrdmb)***

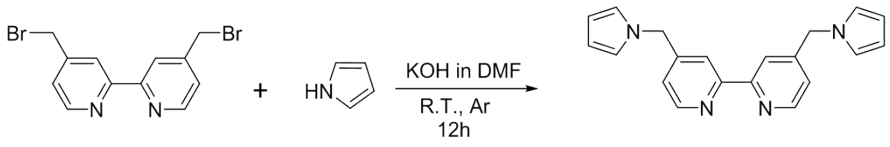

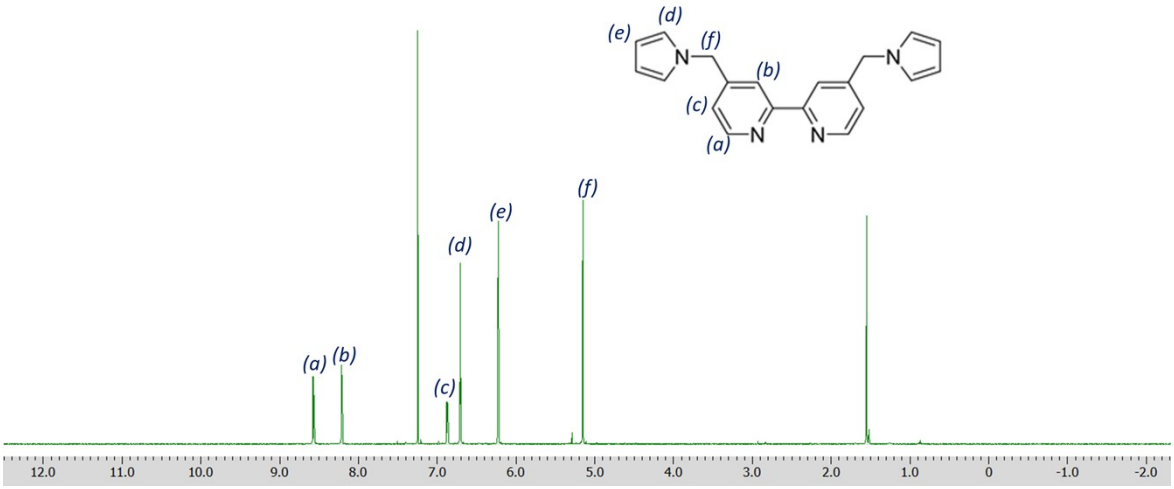

^{1}H NMR spectrum of 4,4'-bis((1H-pyrrol-1-yl)methyl)-2,2'-bipyridine in $CDCl_3$

(b) Synthesis of [Ru(dmb)$_2$]Cl$_2$

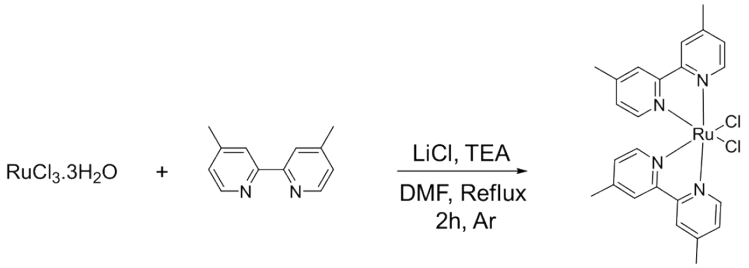

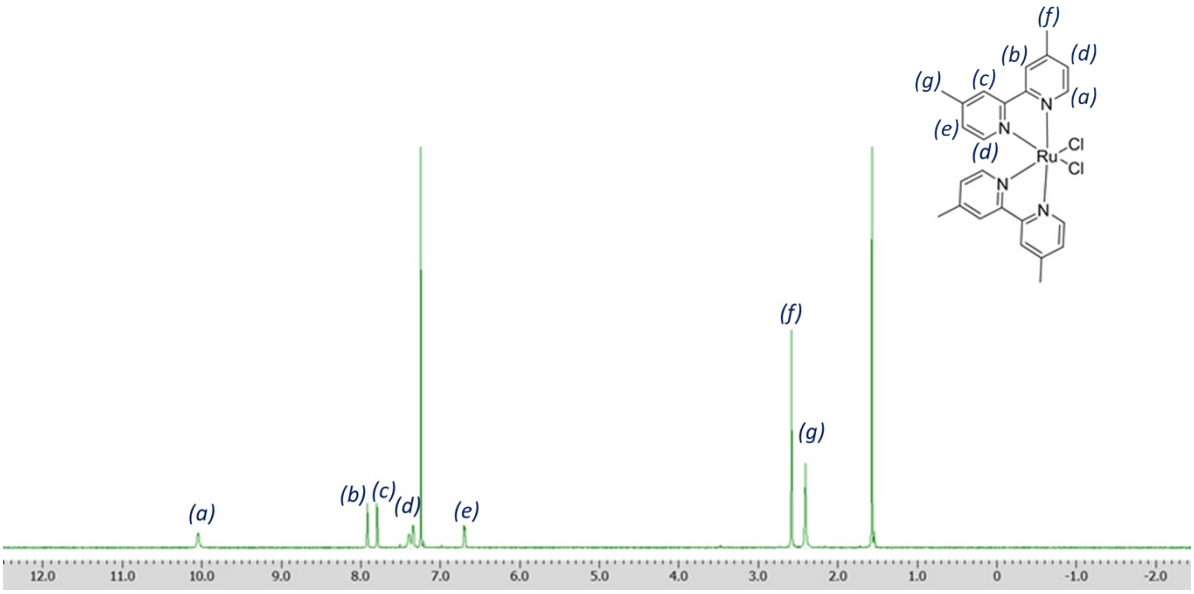

^{1}H NMR spectrum of [Ru(dmb)$_2$Cl$_2$] in CDCl$_3$

(c) Synthesis of [Ru(Pyrdmb)$_2$Cl$_2$]

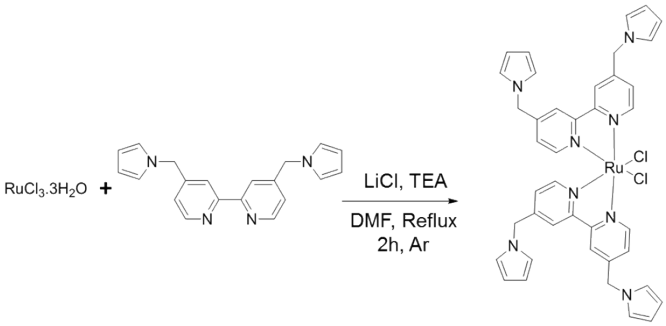

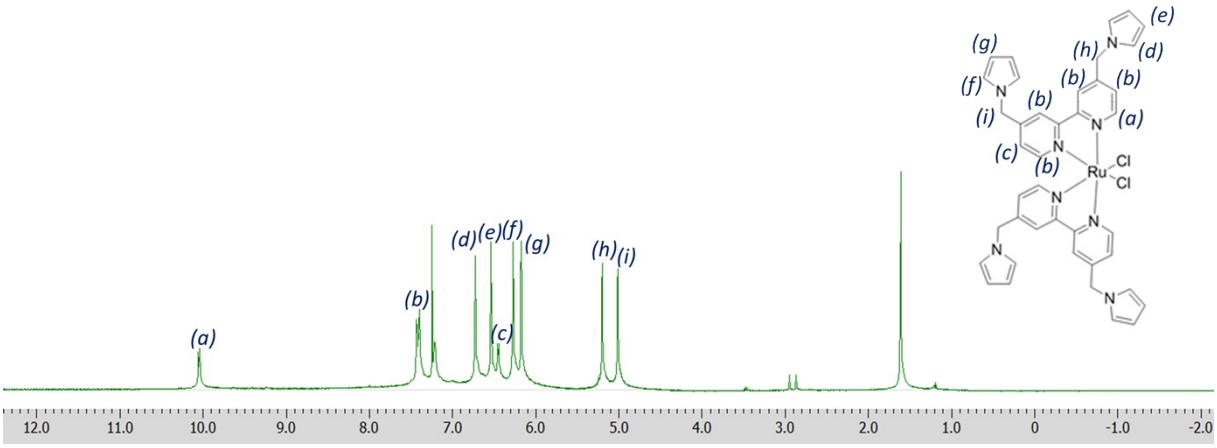

^{1}H NMR spectrum of [Ru(*Pyr*dmb)$_2$Cl$_2$] in $CDCl_3$

(d) Synthesis of [Ru(dmb)(Pyrdmb)Cl$_2$]

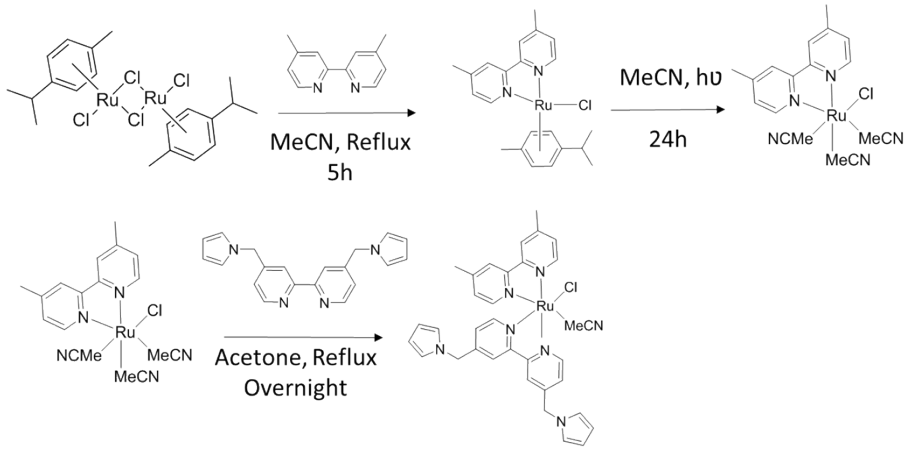

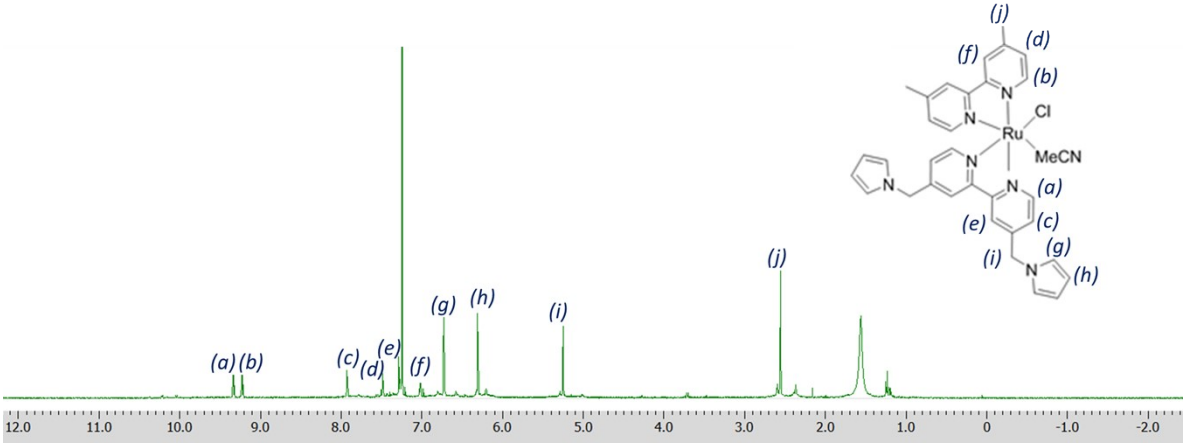

^{1}H NMR spectrum of [Ru(dmb)(*Pyr*dmb)Cl$_2$] in CDCl$_3$

(e) Synthesis of [Ru(dmb)$_2$(Pyrdmb)](PF$_6$)$_2$ (PyrRu)

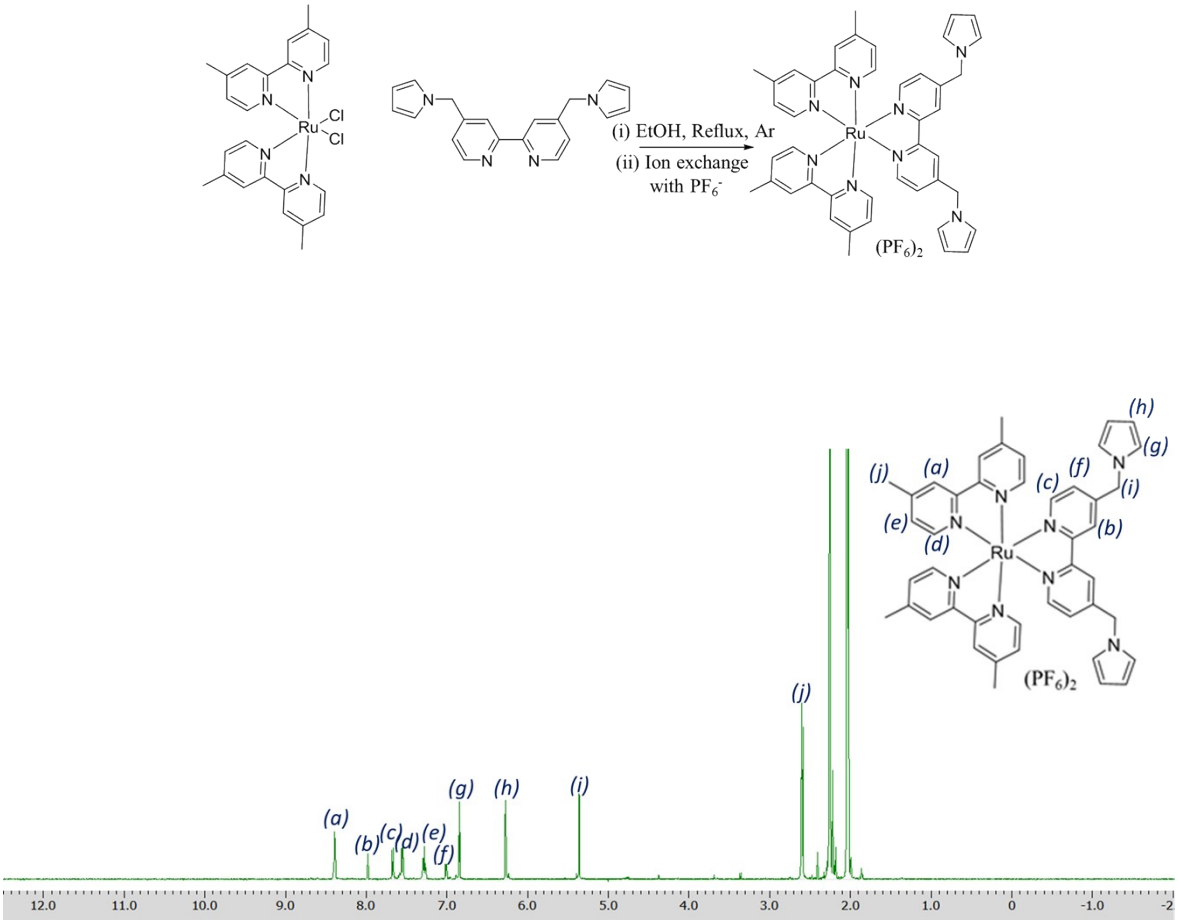

Figure SI-I (5). ^{1}H NMR spectrum of [Ru(dmb)$_2$(*Pyr*dmb)](PF$_6$)$_2$ in Acetone-d$_6$

(f) Synthesis of [Ru(Pyrdmb)$_2$(dmb)](PF$_6$)$_2$ (Pyr2Ru)

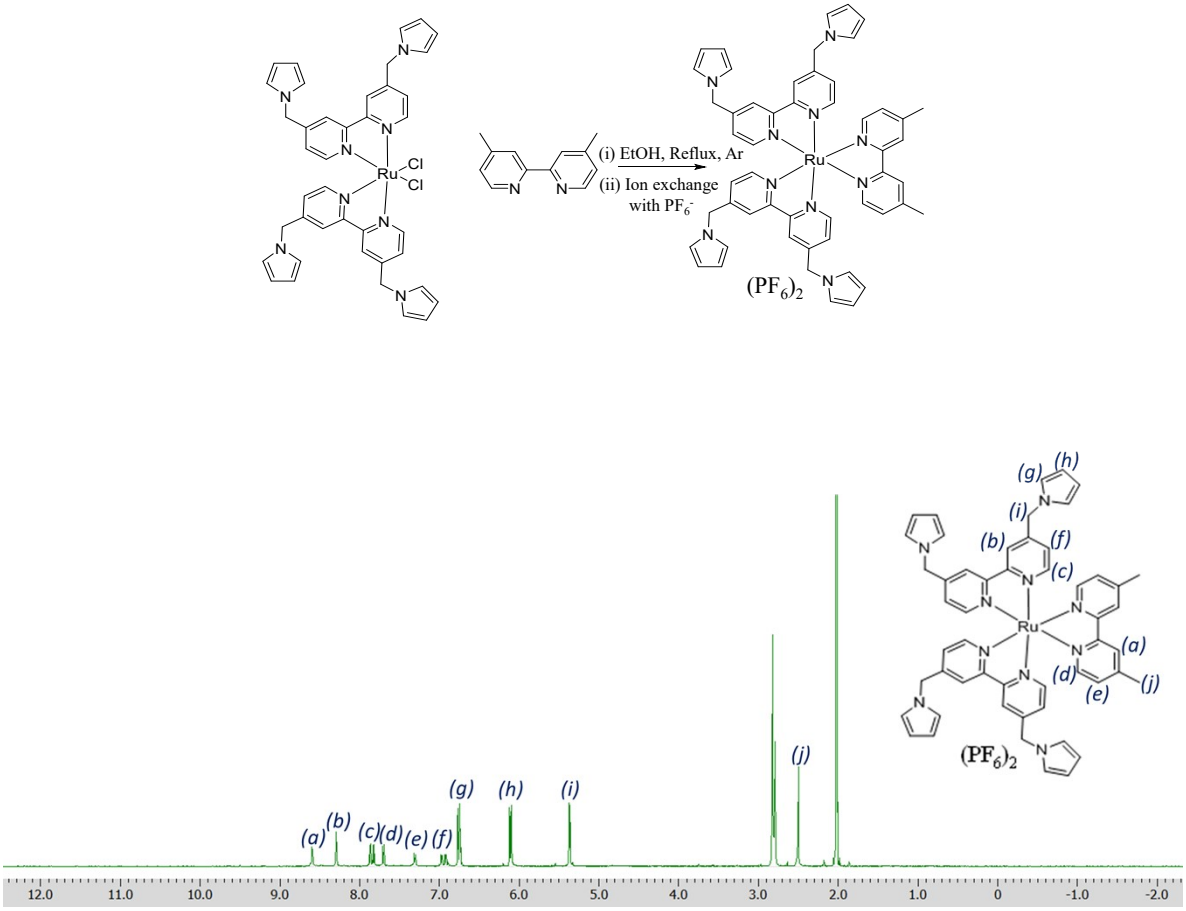

Figure SI-I (6). ^{1}H NMR spectrum of [Ru(*Pyr*dmb)$_2$(dmb)](PF$_6$)$_2$ in Acetone-d$_6$

(g) Synthesis of [Ru(dmb)(Pydmb)(dmb-PO_3H_2)]$(PF_6)_2$ (PRuPyr)

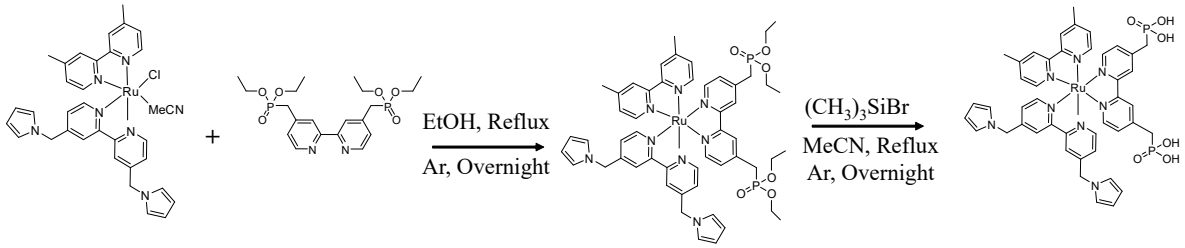

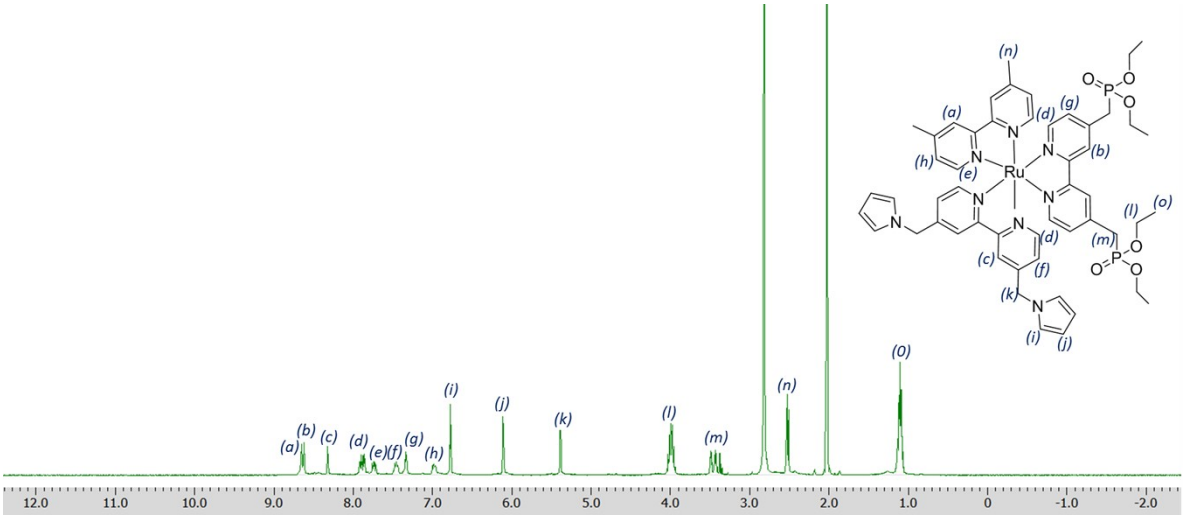

^{1}H NMR spectrum of ([Ru(dmb)(*Pyr*dmb)(dmb-PO_3Et_2)]$(PF_6)_2$ in Acetone-d_6

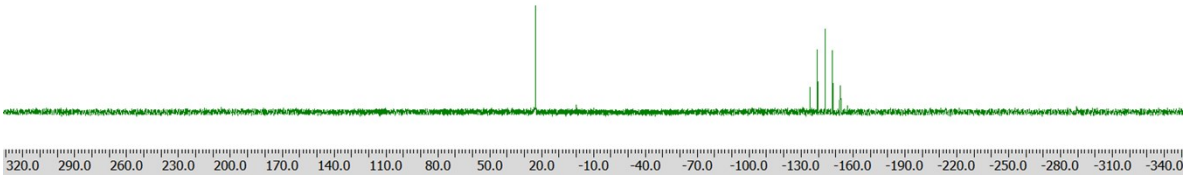

^{31}P NMR spectrum of ([Ru(dmb)(*Pyr*dmb)(dmb-PO_3Et_2)]$(PF_6)_2$ in Acetone-d_6

(h) Synthesis of [Ru(dmb)(Pydmb)(bpyC$_2$bpy)](PF$_6$)$_2$ (PyrRuC$_2$bpy)

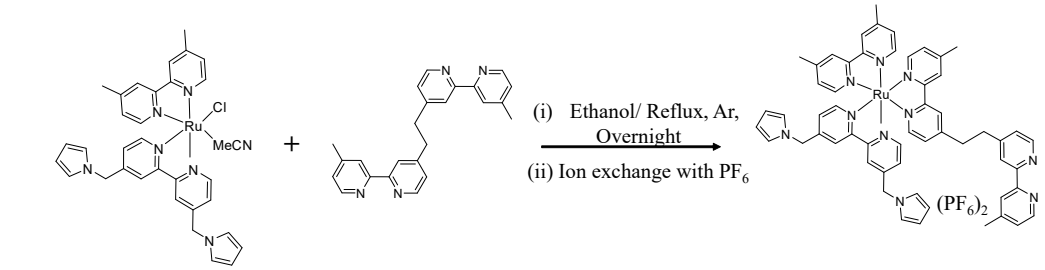

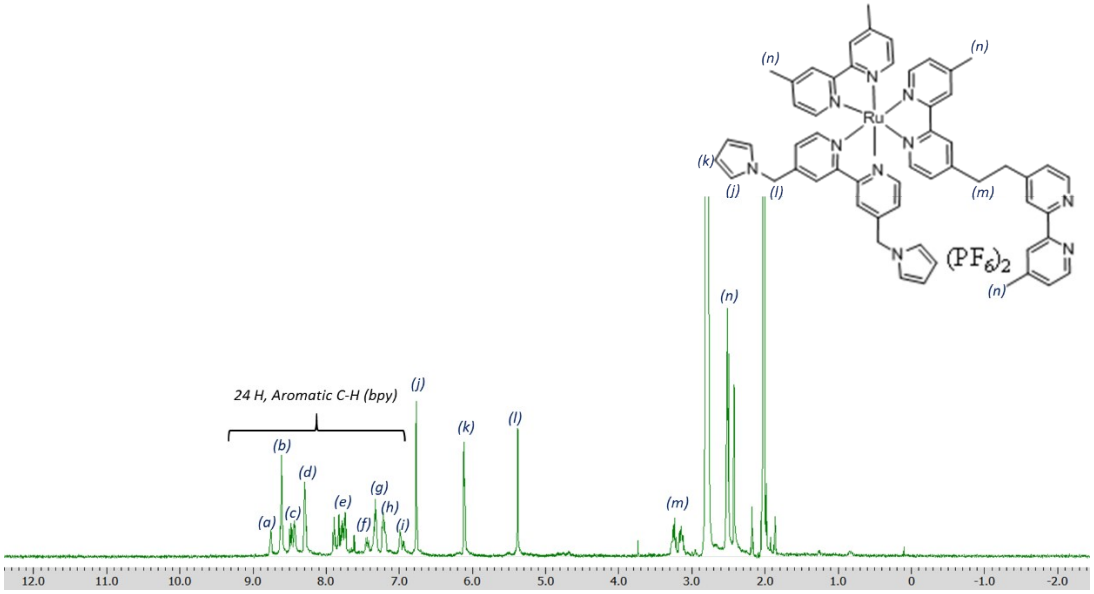

^{1}H NMR spectrum of [Ru(dmb)(*Pyr*dmb)(bpyC$_2$bpy)](PF$_6$)$_2$ in Acetone-d$_6$.

(i) Synthesis of [Ru(dmb)(Pydmb)(bpyC$_2$bpy)Ru(CO)$_2$Cl$_2$](PF$_6$)$_2$ (PyrRuC$_2$RuCAT)

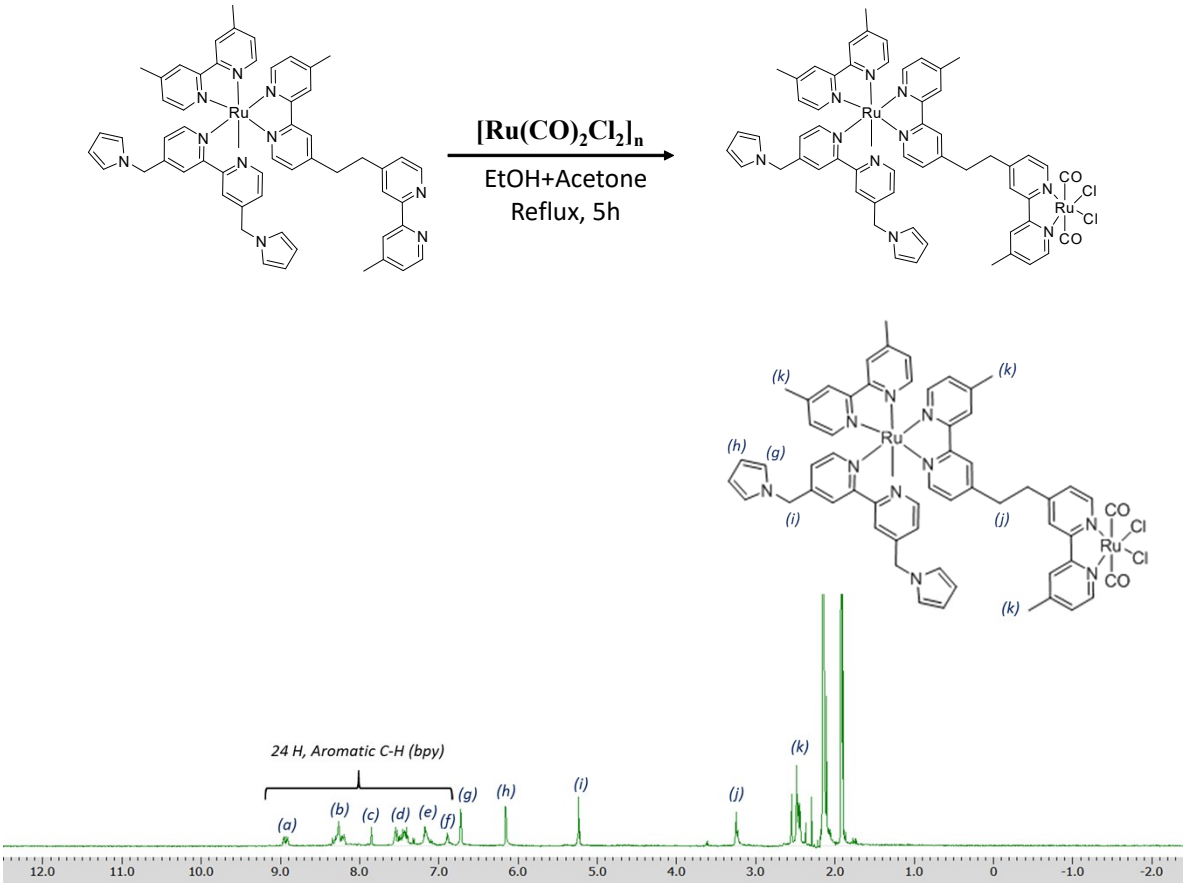

^{1}H NMR spectrum of [Ru(dmb)(*Pyr*dmb)(bpyC$_2$bpy)Ru(CO)$_2$Cl$_2$](PF$_6$)$_2$ in Acetone-d$_6$

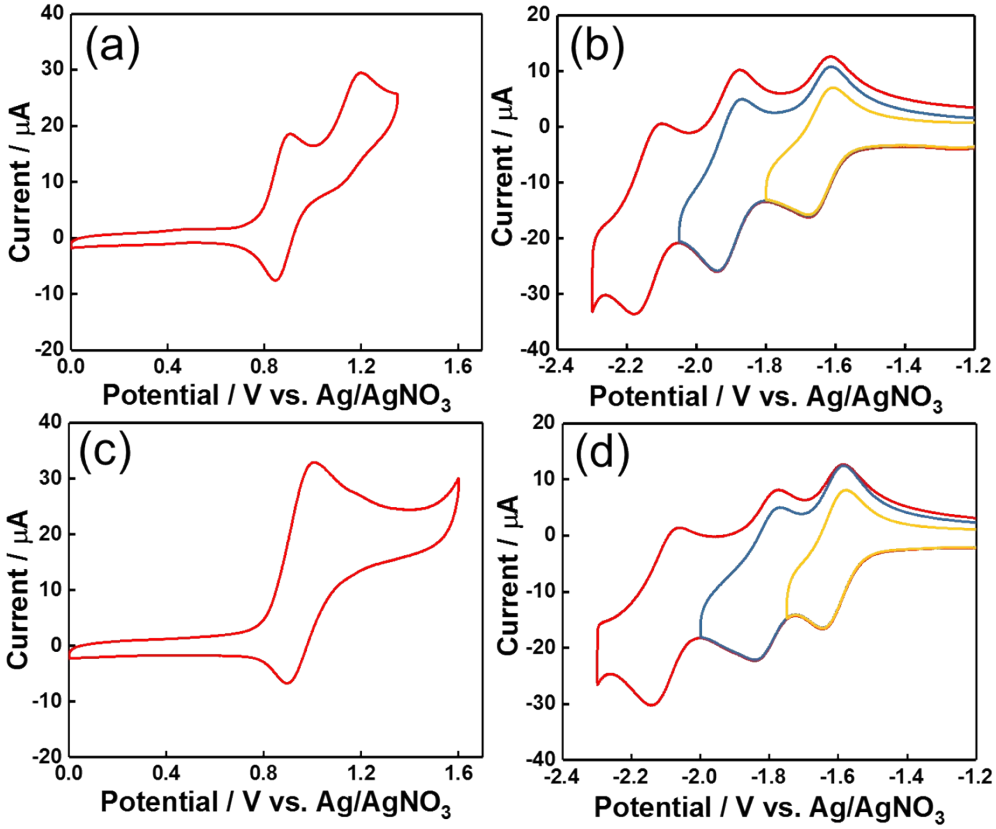

Fig. S1 Cyclic voltammograms of *Pyr*Ru (a, b) and *Pyr2*Ru (c, d) recorded at 200 mV s^{-1} in MeCN containing the corresponding complex (0.5 mM) and Et_4NBF_4 (0.1 M) as the electrolyte under Ar using a ring-shaped glassy carbon working electrode (ϕ = 0.3 mm), a $Ag/AgNO_3$ reference electrode, and a Pt wire counter electrode.

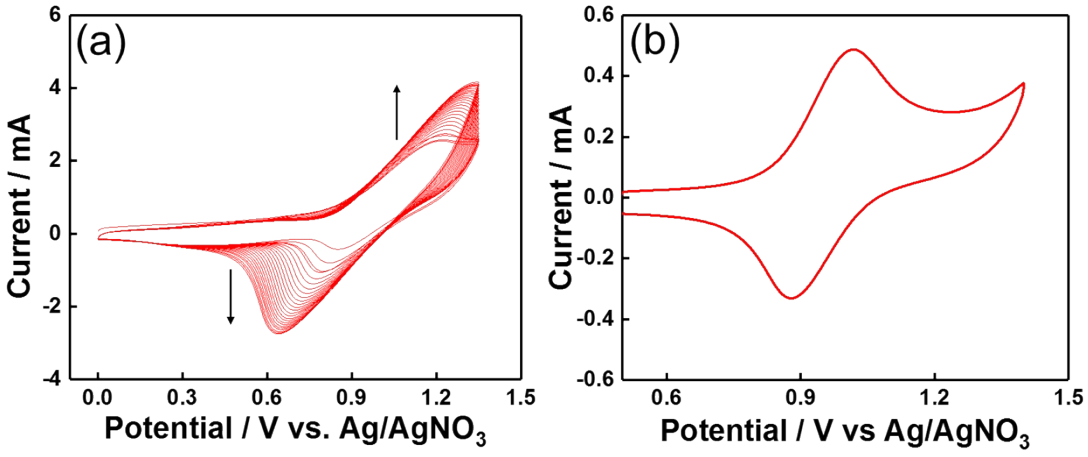

Fig. S2 (a) Cyclic voltammograms recorded during the oxidative electropolymerization of *Pyr2*Ru on NiO (electrode area = 2.5 cm^2) in Ar-saturated MeCN containing *Pyr2*Ru (0.5 mM) and Et_4NBF_4 (0.1 M) as an electrolyte. The potential was cycled 25 times between 0 and +1.35 V (vs. $Ag/AgNO_3$) at 100 mV s^{-1}. (b) Cyclic voltammogram of the NiO/*PolyPyr2*Ru working electrode recorded in MeCN containing 0.1 M Et_4NBF_4 as an electrolyte (counter electrode = Pt coil, reference electrode = $Ag/AgNO_3$) at 10 mV s^{-1}.

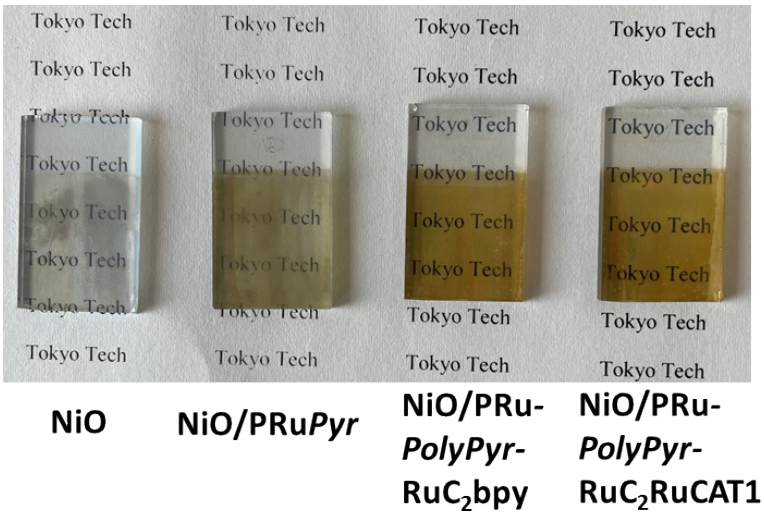

Fig. S3 Images of photocathode after each steps of fabrication

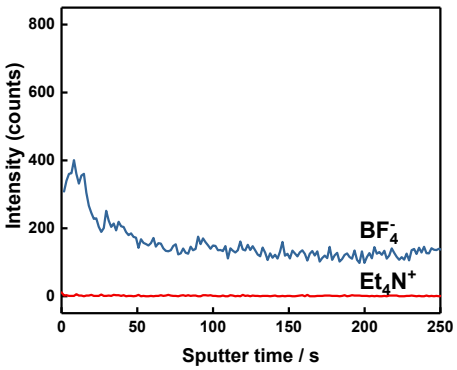

Fig. S4 TOF – SIMS spectra of NiO/PRu-*PolyPyr*-RuC$_2$RuCAT1 for ionic species Et_4N^+ and BF_4^-

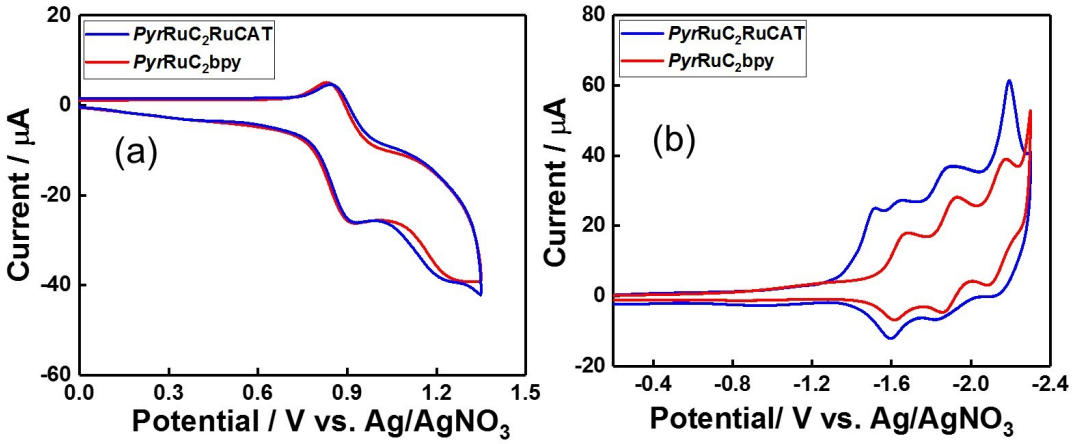

Fig. S5 Cyclic voltammograms of *Pyr*RuC$_2$RuCAT and *Pyr*RuC$_2$bpy measured in MeCN solutions containing 0.1M Et_4NBF_4 as an electrolyte under an Ar atmosphere (Scan rate = 200mV s). WE: GC (ϕ= 0.3mm) RE: Ag/$AgNO_3$ and CE: Pt.

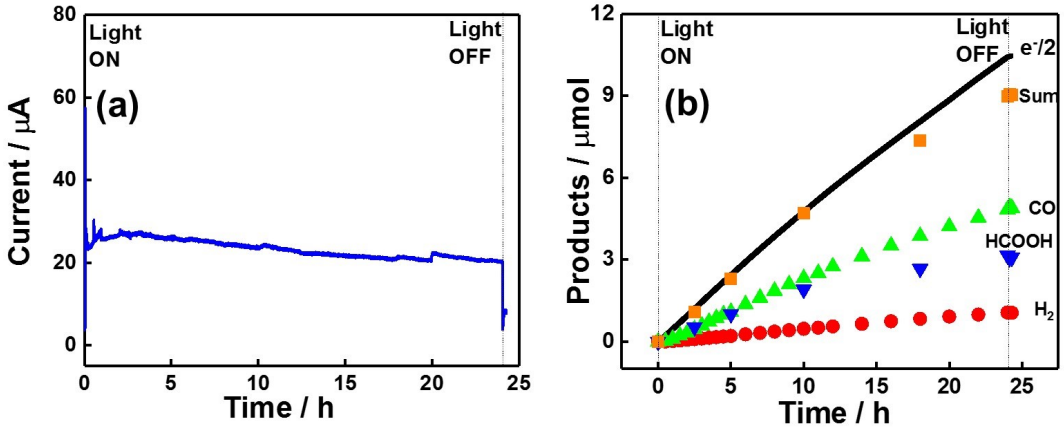

Fig. S6 (a) Time courses of photocurrent and **(b)** products expressed as half of electrons passed (black line), CO (green triangle), HCOOH (blue triangle), and H_2 (red circle). NiO/PRu-*PolyPyr*-RuC_2RuCAT1 (electrode area: 2.5 cm^2) applied bias at E = −0.7 V vs. Ag/AgCl was irradiated at 460 nm < λ_{ex} < 650 nm (8 mW cm^{-2}) in a CO_2-purged 50 mM $NaHCO_3$ aqueous solution (pH = 6.6).

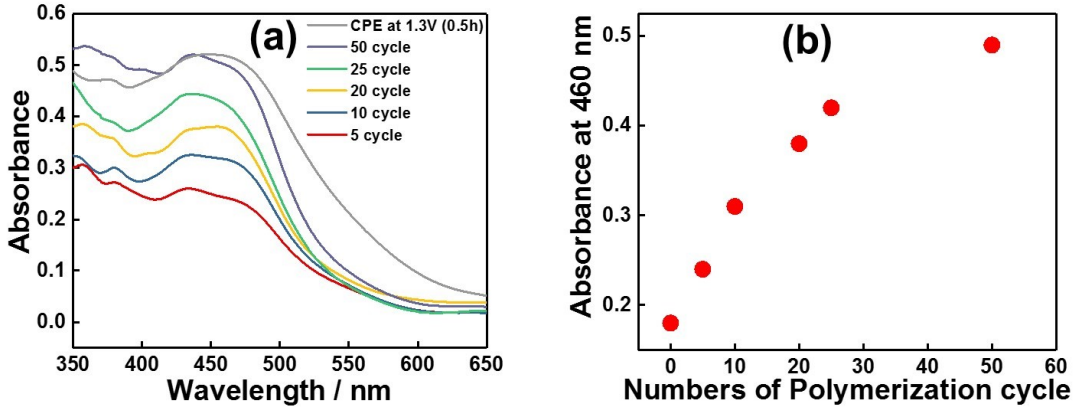

Fig. S7 (a) UV-Vis (DRS) spectra of NiO/PRu-*PolyPyr*-RuC_2RuCAT1 prepared under different number of cycles of oxidative CV scan between 0-+1.35V vs. $Ag/AgNO_3$ **(b)** Plot between absorbance at λ=460 nm versus number of polymerization cycle

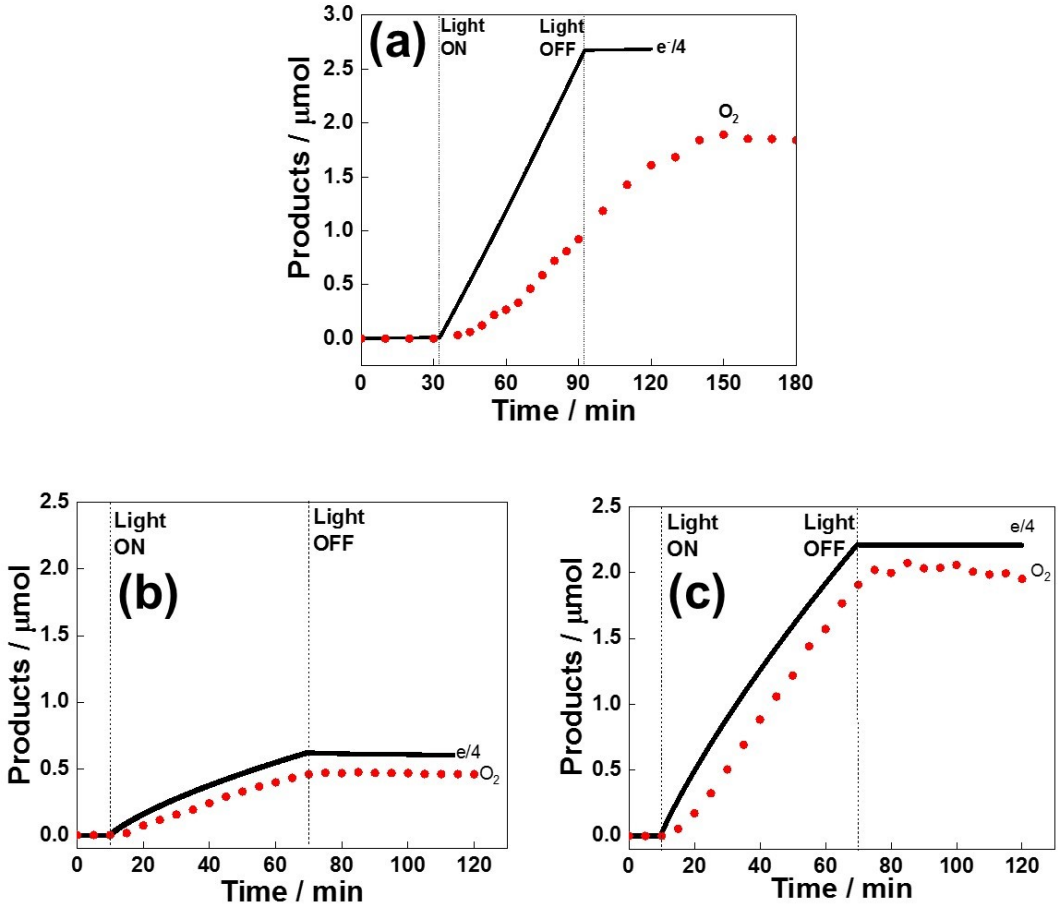

Fig. S8 Time courses of the electrons and oxygen evolved by irradiating $CoO_x/BiVO_4$ or RhO_x/TaON Photoanode in a three-electrode cell with Nafion® membrane in CO_2 purged 50mM $NaHCO_3$ solution by using 400 nm < λ_{ex} < 650 nm (41.2-45.2 mW cm^{-2}) (a) $CoO_x/BiVO_4$ under applied bias 0.0V vs Ag/AgCl (b) RhO_x/TaON under applied bias 0.0V vs Ag/AgCl and (c) RhO_x/TaON under applied bias +0.1V vs Ag/AgCl

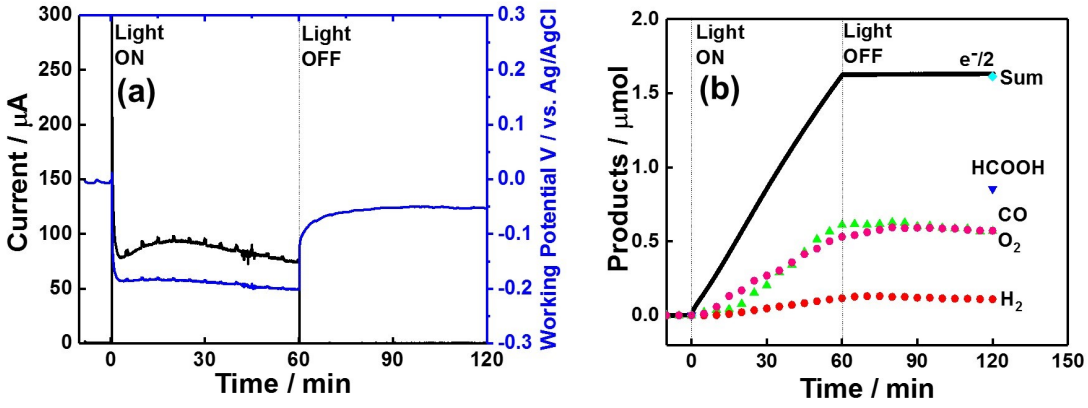

Fig. S9 Construction of artificial Z-Scheme model under simulated sunlight irradiation (AM 1.5) **(a)** photocurrent (black) and working potential of the electrode (blue line) and **(b)** products under simulated solar light irradiation consisting NiO/PRu-*PolyPyr*-$RuC_2RuCAT1$ photocathode and the $CoO_x/BiVO_4$ photoanode without any bias in a CO_2-purged $NaHCO_3$ (50 mM) aqueous solution (pH = 6.6) in a tandem cell configuration.

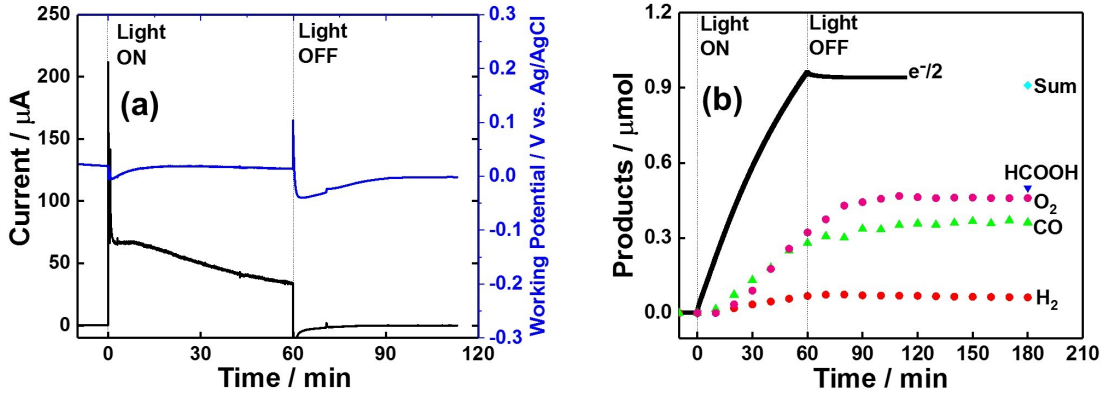

Fig. S10 Construction of artificial Z-Scheme model under simulated sunlight irradiation (AM 1.5) **(a)** photocurrent (black) and working potential of the electrode (blue line) and **(b)** products under simulated solar light irradiation consisting NiO/PRu-*PolyPyr*-$RuC_2RuCAT1$ photocathode and the $RhO_x/TaON$ photoanode without any bias in a CO_2-purged $NaHCO_3$ (50 mM) aqueous solution (pH = 6.6) in a tandem cell configuration.

Table S1 Estimation of PRu*Pyr* on NiO/PRu*Pyr* by ICP-MS method (Step – 1)

Sample No	Total amount of PRu*Pyr* n_{PRuPyr} (nmol)
1	16.7
2	15.9
3	13.0
4	16.5

Average amount of PRu*Pyr* adsorbed (n_{PRuPyr}) = 15.5 ± 1.3 nmol

Table S2 Estimation of total Ru Photosensitizers (RuPS) by ICP-MS analysis of NiO/PRu-*PolyPyr*-RuC_2bpy (Step – 2)

Sample No	Total amount of Ru photosensitizer n_{RuPS} (nmol)
1	76.1
2	73.2
3	77.2
4	75.1

Average amount of RuPS adsorbed = 75.4 ± 1.3 nmol

Table S3 Estimation of total amount of Ru (PS+CAT) by ICP-MS analysis of NiO/PRu-*PolyPyr*-RuC_2RuCAT1 (Step – 3)

Sample No	Total amount Of Ru $n_{Ru(PS+CAT)}$ (nmol)
1	109.5
2	103.9
3	92.5
4	95.2

Average amount of Ru(PS+CAT) adsorbed = 100.3 ± 5.5 nmol

Table S4 Estimation of total amount of Ru (PS+CAT) by ICP-MS analysis of NiO/PRu-*PolyPyr*-RuC_2RuCAT2 (Two-step method)

Sample No	Total amount Of Ru $n_{Ru(PS+CAT)}$ (nmol)
1	49.2
2	34.6
3	35.5
4	43.4
Average amount of Ru(PS+CAT) adsorbed = 40.7 ± 5.6 nmol	

Table S5 Photoelectrochemical reactions using NiO/PRu-*PolyPyr*-RuC_2RuCAT1 under varying conditions for 5h.

Entry	Applied Potential	Light	Atmosphere	Electrolyte	Products / µmol			
					$e^-/2$	CO	HCOOH	H_2
1	O	O	CO_2	$NaHCO_3$	4.6	2.9	1.1	0.3
2	O	X[a]	CO_2	$NaHCO_3$	n.d.	n.d.	n.d.	n.d.
3	X[b]	O	CO_2	$NaHCO_3$	n.d.	n.d.	n.d.	n.d.
4	O	O	Ar	Phosphate[c]	06	n.d.	n.d.	0.1

[a] Without irradiation. [b] Without potentiostat. [c] Phosphate buffer: pH 7.4, [$Na_2HPO_4.7H_2O$] = 75.4 mM + [$NaH_2PO_4.H_2O$] = 24.6 mM.